Sensing the human body by implanted RFID tags

[1]C. Occhiuzzi, [2]G. Marrocco

DISP, -University of Roma Tor Vergata
Via del Politecnico,1, 00133, Roma (ITALY)
[1]occhiuzzi@disp.uniroma2.it
[2]marrocco@disp.uniroma2.it

***Abstract*—Starting from the physical evidence that passive RFID systems may be used as self-sensing devices, the feasibility of human monitoring by means of implanted tags is here investigated. The sensing capabilities, the backscattering contrast and the communication link are analyzed considering a specific medical application, i.e. the continuous monitoring of brain edema evolution in patients neurosurgery treated. By using numerical simulations all the significant issues of the passive sensing are here investigated at different frequency bands. Preliminary experimental results with simplified phantoms corroborate the analysis.**

I. Introduction

Beside the common logistic usages of the Radio Frequency Identification (RFID) technology, one of the most innovative and promising applications is the possibility to process the backscattering signals with the purpose to detect additional information about the target, such as its state and its evolution, without any specific embedded sensor or local power supply. The rationale of this idea lies in the clear dependence of the tag's input impedance and radar cross section on the physical and geometrical features of a real target. When the object where the tag is attached on undergoes some changes along with the time, the tag's electrical features also change and these variations can be remotely detected by the reader [1].
The possibility to remotely monitor processes in evolution opens interesting opportunity in telemedicine and human health monitoring in general, especially concerning implantable devices. One or more battery-less RFID radio-sensors could be implanted inside the human body in close proximity, for example, to a surgery treated region and interrogated by an external reader. Based on the sensors response at different times (days or even hours) a map of the geometrical or chemical changes of the tissues could be produced, thus evaluating the healing process and possible complications, e.g. abnormal cell proliferations, edema and inflammatory events (Fig. 1).
A possible application of the proposed sensing platform is the monitoring of brain edema evolution after surgical treatment of brain cancer [2]. The edema results from the flow of fluid into the extracellular space of the brain parenchyma and produces an increase of the intracranial pressure. This pathology causes high grade symptoms: reduction in cerebral blood flow, nausea, vomiting, neurological disorders and in its most severe form, the widespread ischemia. The differential diagnosis of the edema progression is actually possible only with CT scan or NMR. These imaging analysis are not frequently used, due to their cost and availability, especially for some EU and no-EU countries.

Starting from the physical evidence for which the peritumoral tissues gradually absorb the liquid, consequently modifying their electromagnetic characteristics [3], the aim of this study is to check the feasibility of the system especially in term of sensing capabilities, backscattering contrast and communication link. By using numerical simulations (FDTD modeling) the passive sensing from implanted RFID systems is here investigated at different frequency bands. A monochromatic analysis around $870MHz$ and $250MHz$ permits to discuss the expected performance of conventional UHF and microwave RFID systems, while an impulsive analysis is applied to understand the physical potentiality of an ultra wideband interrogation. An early experimental validation corroborate the sensing approach and the reasonableness of the proposed platform.
Although all the following discussion is specific to the brain's edema problem, a similar methodology may be applied to other body regions, as it will shown at the Symposium.

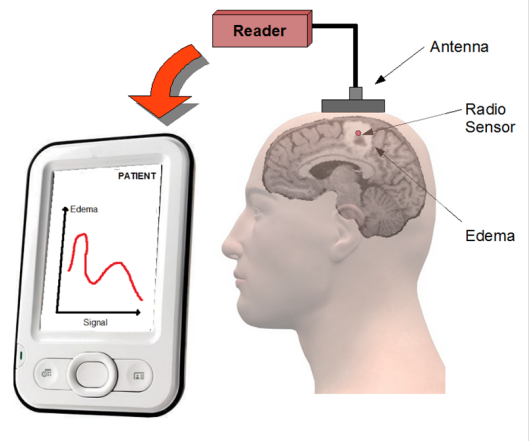

Fig. 1. A possible set-up for the wireless monitoring of brain edema by implanted RFID technology.

II. RFID-Sensing Equations

We generally denote with Ψ a physical or geometrical parameter of the target which has to be monitored by the RFID platform. For the specific application Ψ will be a shape factor of the edema.

The two-way reader-tag link may be hence rewritten making explicit the dependence on object's physics. The power collected at the microchip (1) and the power backscattered by the tag toward the reader (2) and collected by this are:

$$P_{R\rightarrow T} = \left(\frac{\lambda_0}{4\pi d}\right)^2 P_{in} G_R(\theta,\phi) G_T(\theta,\phi,\Psi(t)) \tau(\Psi(t)) \eta_p \tag{1}$$

$$P_{R\leftarrow T} = \frac{1}{4\pi}\left(\frac{\lambda_0}{4\pi d}\right)^2 G_R(\theta,\phi)\eta_p^2\, rcs_T(\theta,\phi,\Psi(t)) \tag{2}$$

where d is the reader-tag distance, $G_R(\theta,\phi)$ is the gain of the reader antenna, $G_T(\theta,\phi,\Psi(t))$ is the gain of the tag's antenna when placed on the target. P_{in} is the power entering in the reader antenna, η_p is the polarization mismatch between the reader and the tag, $\tau(\Psi(t))$ is the power transmission coefficient of the tag.

$$\tau = \frac{4R_{chip}R_A(\Psi(t))}{|Z_{chip}+Z_A(\Psi(t))|^2} \tag{3}$$

rcs_T is the tag's radar cross-section, related to the modulation impedance Z_{mod} of the microchip to encode the low and high digital state:

$$rcs_T = \frac{\lambda_0^2}{4\pi} G_T^2(\theta,\phi,\Psi(t)) \left(\frac{2R_A(\Psi(t))}{|Z_{mod}+Z_A(\Psi(t))|}\right)^2 \tag{4}$$

The backscattered power $P_{R\leftarrow T}$, directly measurable by the reader, is therefore strictly correlated to the physical variation of the tagged object through the change of impedance and gain of the tag. In particular, when the reader-tag mutual position remains the same in successive interrogations, it is possible to simply derive a *measurement curve* $p_s \leftrightarrow \Psi(t)$, independent on the reader-tag distance and reader's gain, by referring the backscattered power to a particular state Ψ_0 of the object:

$$p_S(\Psi) \equiv \frac{P_{R\leftarrow T}(\Psi)}{P_{R\leftarrow T}(\Psi_0)} = \frac{rcs_T(\theta',\phi')[\Psi]}{rcs_T(\theta',\phi')[\Psi_0]} \tag{5}$$

Alternative processing algorithms for random reader-tag mutual position will be shown at the Symposium.

III. Edema Model

The electromagnetic characteristics of the implanted antenna are numerically analyzed using the Finite Difference Time Domain (FDTD) method. The head has been modeled as a multilayered lossy dielectric hemisphere, whose external and internal sizes reproduce with good approximation the real human districts (Fig.2). Each layer of the model is characterized by its specific dielectric properties (given in Table I). The tag is modeled as a 1cm-long coated dipole and it is fully immersed in the center of the edema.

Due to the surgical removal of the tumor a dump of blood is expected to invade immediately the treated area (condition t_0 in Fig. 2). After a variable period, due to the surgery and other possible tumoral complications, an edema could arise and advance around the surgical tissues, modifying their water content and thus their dielectric properties.

The edema evolution is modeled by gradually varying the extension of a circular area concentric with the tumor (conditions t_1, t_2, t_3 in Fig.2), such that the edema radius increases from $0cm$ (no edema) to $0.8cm$.

	870MHz		2.4GHz	
	ϵ_r	σ [S/m]	ϵ_r	σ [S/m]
Skin	41	0.85	38	1.46
Fat	5.46	0.05	5.28	0.1
Bone	12.48	0.14	11.38	0.39
Dura	44.5	0.95	42.03	1.67
Liquor	68.7	2.4	66.24	3.46
Grey Matter	52.87	0.93	48.91	1.81
White Matter	39	0.58	36.17	1.21
Blood	61.46	1.52	58.26	2.55
Edema	50.25	1.0	48.5	1.65

TABLE I
Dielectric properties of human tissues at $f = 870MHz$ and $f = 2.4GHz$

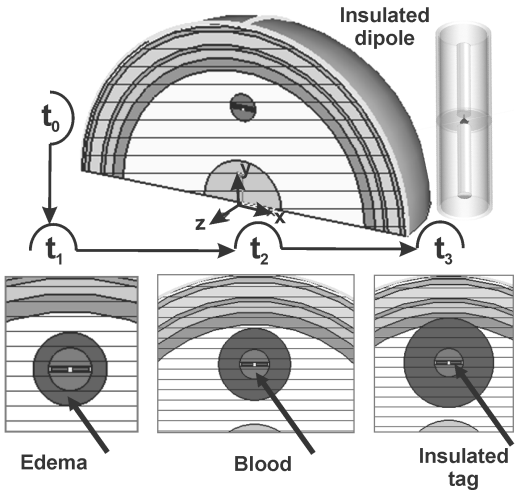

Fig. 2. FDTD model of the edema evolution. The edema is modeled as a variable circular area around the excited tumor.The tag is a 1cm-long coated dipole

Particular attention has been devoted to the definition of edema dielectric properties since up to date only few works are available in the open scientific literature. A generic theoretical model [4] has been adopted elaborating the proposed empirical equations valid over a $0.01-17GHz$ frequency range:

$$\epsilon_r = 1.71 f^{-1.13} + \frac{[\epsilon_S^m - 4]}{1+(f/25)^2}] + 4 \tag{6}$$

$$\sigma = 1.35 f^{0.13}\sigma_{0.1} + \frac{[0.0222(\epsilon_S^m - 4)f^2]}{1+(f/25)^2}] \tag{7}$$

with f frequency of operation in GHz and ϵ_S^m and $\sigma_{0.1}$ empirical coefficients dependent on the tissue water content.

The edema has been thus considered as normal white matter with an anomalous 80% water content (Fig.3). Position and

size of the tumor has been chosen considering data produced by human computer tomographies (CT) of typical pathologies.

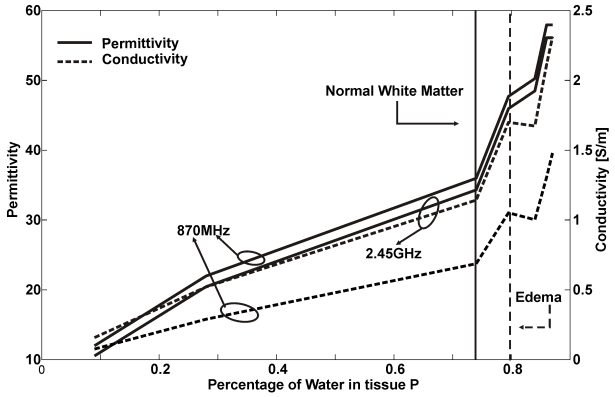

Fig. 3. Dielectric properties of white matter varying its percentage of water.

IV. Narrowband Analysis

Simulations show that the input impedance of the dipole is very little sensitive to the edema evolution (see Fig.4) and in first approximation it may be considered constant all along the phenomenon. In the initial condition t_0, the maximum gain G_{0Max} achieved along the y-axis in Fig.2 is $-31dB$ for $870MHz$ and -29.7 for $2.45GHz$. Unlike the input impedance, for both RFID frequencies the gain is quite affected by the edema evolution, as pointed out in Tab.II

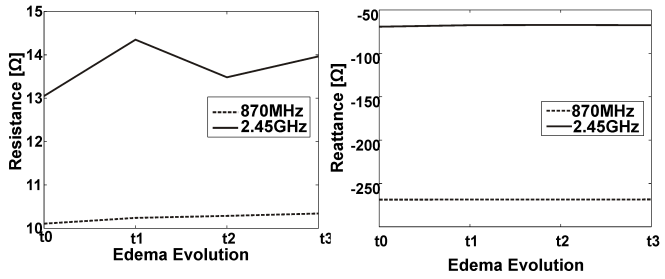

Fig. 4. Input impedance of the implanted dipole with edema evolution.

	t_0	t_1	t_2	t_3
$870MHz$	-31	-30.9	-31.1	-31.3
$2.45GHz$	-29.7	-29.8	-30.0	-30.5

TABLE II
Maximum Gain $[dB]$

Consequently, the backscattering power ratio $p_S(\Psi)$ from (4) and (5) becomes

$$p_S = \frac{G_T^2(\theta, \phi, \Psi)}{G_T^2(\theta, \phi, \Psi_0)} \tag{8}$$

Having fixed the reader-tag mutual position in the direction of maximum gain, the computed backscattered power ratio p_S referred to the initial condition t_0 is shown in Fig. 5. For both RFID frequencies the curves are nearly monotone with the edema evolution. The overall variation is about 15% for $870MHz$ and 35% for $2.45GHz$. The response at $2.45GHz$ is more affected by the edema growth than the $870MHz$ one due to the larger electromagnetic size of the edema at the higher frequencies. However, body attenuation at $2.45GHz$ is expected to be much more significant, practically reducing the power harvested by the microchip, so making the tag's awakening more critical. When a regular RFID link is assumed, involving a reader which emits $3.2W$ EIRP, e.g. the maximum allowed by European regulations, the power collected by the implanted tag, under the hypothesis of ideal impedance matching, can be estimated by eq.(1). Considering a distance $d = 4.3cm$, at $870MHz$ the power received by the internal dipole approximately ranges between 1.50 and $1.40mW$. At $2.45GHz$ the power level decreases to 0.72 and $0.58mW$. The communication link can be therefore achievable since the power absorbed by the implanted tag exceeds the actual commercial tag's microchip sensitivity threshold p_T (currently of the order of some μW). The simulation results indicate that the sensitivity of the external reader should be less than -50dB to detect the sensing signal, as it is generally verified in actual commercial readers (sensitivity $\sim -100dBm$).

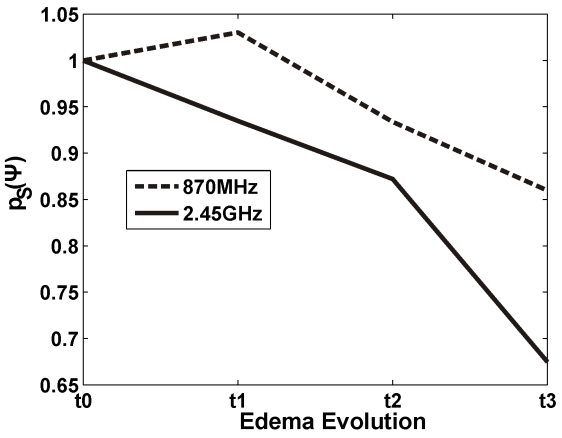

Fig. 5. Backscattering power ratio of the dipole.

A very preliminary experimental validation is visible in Fig.6, where a planar T-matched dipole, attached over a box filled with a liquid phantom of variable level, is continuously interrogated by a fixed reader. The water level was changed from $h_W = 0cm$ to $h_W = 8cm$. Like the simulation results, the backscattered power ratio p_S changes as the liquid level increases, with a nearly monotone 10dB dynamics (except for a very early condition $h_W < 2cm$). In the linear range the slope is about 1.5 and hence a 1cm-variation of the water level is sensed as a 15% change in the measured data.

Although this experimental setup is very rough and far from a realistic brain edema model, it is a first check of the sensing approach and corroborates the reasonableness of the sensing

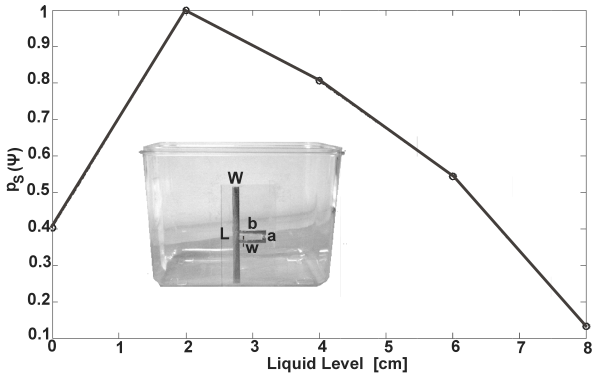

Fig. 6. Measured backscattering power ratio of the T-matched dipole (size in [mm] $L = 80, W = 5, a = 10, b = 20.26, w = 3$) placed on a liquid phantom box (size in [mm] $140 \times 90 \times 110$)

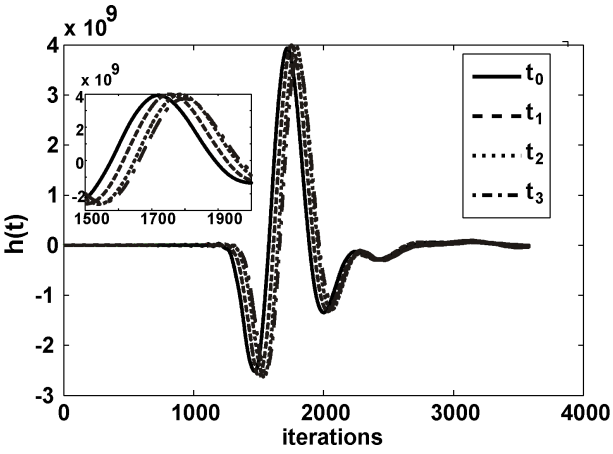

Fig. 7. Effective height $h(t)$ of the implanted dipole

concept.

V. UWB Analysis

The analysis of the implanted tag response to Ultra wideband interrogation is again performed by considering the tag in transmitting mode. The dipole's gap is sourced by a differentiated Gaussian pulse $x_G(t)$ of unitary peak value and maximum frequency of about $15GHz$. The frequency dispersion of the different healthy and unhealthy cerebral tissues is properly included in FDTD simulations according to the model in [5].

The behavior of the tag during the edema evolution is analyzed through the concept of antenna impulse response which is independent on the particular interrogation waveform or interrogating antenna. At this purpose, denoting with $E_\xi(\underline{r}_0, t)$ the $\xi = \{x, y, z\}$ component of time-varying electric field radiated by the implanted antenna at point $\underline{r}_0$ outside the head, the antenna impulse response $h_\xi(t, \underline{r}_0)$ is calculated by deconvolving the excitation signal $x_G(t)$ out of $E_\xi(\underline{r}_0, t)$, e.g.

$$h_\xi(\underline{r}_0, t) = x(t) \otimes \underline{E}_\xi(\underline{r}_0, t) \tag{9}$$

The Gaussian deconvolution is numerically performed by the Moment Expansion method in [7]. It is worth noticing that the impulse response includes the effect of tag's shape but also the electromagnetic interaction with the living tissues which are rather lossy. This means that although the implanted dipole is not broadband itself, the presence of lossy tissues will make the transmitted wavepacket rather concentrated in time, simplifying the detection.

Fig.7 shows the x-component of the impulse response at 0.5cm from the head's surface, in correspondence to the y-axis (see Fig.2).

The edema evolution primarily produces a linear time shift of the signals with respect to the initial condition. The attenuation effects are instead not significant. The presence of the time shift can be related to the different propagation paths of the fields inside the head caused by the edema evolution. Due to an increased water content, the dielectric permittivity of the edema is sensibly different from the healthy tissue, as shown in Fig.8, with variation $\Delta\epsilon_r = \epsilon_{rEdema} - \epsilon_{rWhite} \sim 10$ which stays approximately constant in the entire band. The edema-filled region is hence electrically wider than the white matter one, therefore introducing an increasing delay in the field propagation.

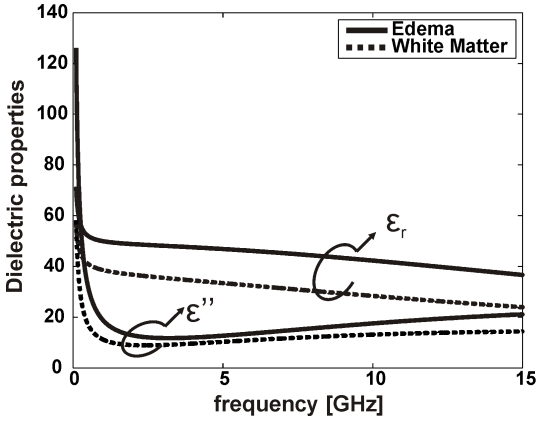

Fig. 8. Dielectric property of normal and edematous white matter in the entire frequency range

It is possible to appreciate in Fig.9 that the time-delay of the signals' peak is rather monotone with the edema evolution, so promising the possibility of a remote detection capability.

VI. Conclusions

The investigated RFID in-body monitoring could provide various degrees of freedom which may be used to collect information about the patient's state during the surgery follow-up. Both narrowband and ultra-wideband analysis seems to demonstrate that the edema evolution produces specific and macroscopic effects to the electromagnetic response of the tag which are nearly monotonic with the physical phenomenon and that could be collected and measured by available technology. In particular narrowband sounding (involving standard RFID protocols) and UWB interrogations could be merged

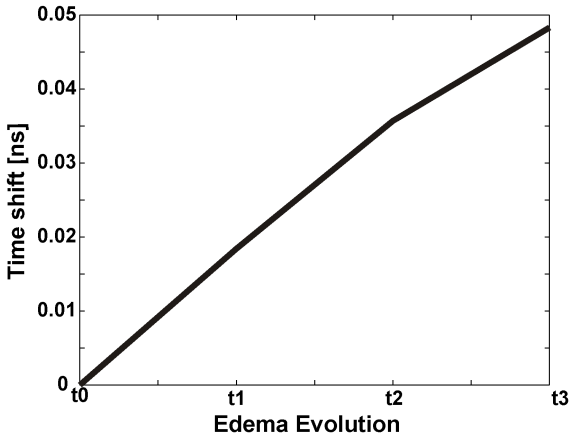

Fig. 9. Time shift of the signal peaks referred to the initial condition t_0

together by data fusion algorithms to improve the sensitivity or even to collect multi-dimensional informations about edema evolution.

The presented results are no-antenna specific: a possible implantable tag could be for example a miniaturized helical-antenna which offers good performances in term of dimensions, integrability and sensing capabilities. A more realistic experimental validation is at the moment in progress.

ACKNOWLEDGMENT

The authors wish to thank prof. Alfredo Marinelli of the Oncology Department of the University of Naples "'Federico II"', for inspiration and discussions.

REFERENCES

[1] G. Marrocco, L. Mattioni, C. Calabrese, "'Multi-port Sensor RFIDs for Wireless Passive Sensing - Basic Theory and Early Simulations"', *IEEE Trans. Antennas Propagation.*. vol.56, n.8, pp.2691-2702, Aug. 2008

[2] M. Bitzer, T. Nagele, B. Geist-Barth, Uwe Klose,Eckardt Gronewaller, Matthias Morgalla, Eckart Heiss, and KarstenVoigt, Role of hydrodynamic processes in the pathogenesis of pritumoralbrain edema in meningioma, J Neurosug,93594-604,2000

[3] H. Pin Kao, E. R.Cardoso,E. Shwedyk, "Correlation of Permittivity and Water Content During Cerebral Edema", *IEEE Transaction on Biomedical Engineering* VOL. 46, NO. 9, September 1999

[4] J. L Schepps, K. R Foster, "The UHF and microwave dielectric properties of normal and tumour tissues: variation in dielectric properties with tissue water content", *Phys. Med. Biol.*, 1980, Vol. 25. No. 6, 1149-1159.

[5] C.Gabriel and S.Gabriel, "Compilation of the Dielectric Properties of Body Tissues at RF and Microwave Frequencies", Internet document; URL: http://niremf.ifac.cnr.it/docs/DIELECTRIC/home.html

[6] A.Shlivinski,E. Heyman,R.Kastner,"'Antenna Characterization in the Time Domain"', *IEEE Transaction on Antennas and Propagation*, VOL. 45, NO. 7, JULY 1997

[7] G. Marrocco, F. Bardati, "'FDTD computation of microwave device impulse response"', *Electronics Letters*,vol.35, n.3,pp223-224, 1999.